Active Cancellation Stealth Analysis Based on Cancellaty

Mingxu Yi[1]**, Lifeng Wang**[1,2]**, Yalin Pan**[1] **and Jun Huang**[1]

Abstract: Active cancellation stealth is a significant developing direction in modern stealth technology field. In this paper, according to characteristics of linear frequency modulated (LFM) signal and nonlinear frequency modulated (NLFM) signal, the cancellation signal was designed. An important parameter called cancellaty which is used to measure the effect of cancellation is proposed. The basic theory of active cancellation stealth is introduced. Based on radar target fluctuation models, the formulas of the radar detection probability are given. Combining the definition of cancellaty with radar detection probability, the effective scope of the cancellaty is ensured. Simulation results show the effectiveness and the practicability of active cancellation.

Keywords: Active cancellation, linear frequency modulation (LFM), nonlinear frequency modulation (NLFM), detection probability, signal-to-noise ratio (SNR).

1   Introduction

In modern world, stealth technology is a comprehensive technology, the military used it to reduce all kinds of observational features of weapon system, so that the detector can not find the target, or make the detection distance shortened [Lynch (2004); Kay and Boudreaux-Bartels (1985); Mauro, Rafael and Mirabel (2007); Jenn (2005)]. Stealth technology including the reduction of radar, infrared, acoustic characteristic features of aircraft. Reducing the radar feature is mainly reduce the target's radar cross section (RCS). Radar target (airplane, ship or tank) stealth technology can be divided into passive and active stealth. In contrast with passive technique, the target radar detection probability could be reduced further by active technique [Qu and Xiang (2010); Xiang, Qu, Li and Hou (2013); Qu, Xiang, Hou and Zhou (2011); Xiang, Qu, Ping and Zhao (2010)]. Active cancellation stealth technique is that the radar target using its loading active equipment to emit inverted echo, and cancelling true target echo at the radar receiving antenna, and then

---

[1] School of Aeronautic Science and Technology, Beihang University , Beijing, China.

[2] Corresponding author.

reducing the radar received true target echo.

Two signals in free space generate coherent interference which makes the synthesized signal weaker or stronger. During the investigation of signal cancellation, more attention has been paid to radar interference signal or clutter [Guo, Sun and Yeo (2008); lizuka, Freundorfer and Iwasaki (1989); Root (1998)], acoustic signal [Paleologu and Benesty (2014); Cecchi, Romoli, Peretti and Piazza (2012); Stanciu and Benesty (2013)], linear frequency modulation pulse compression signal [Wang, Zhao and Wang (2008); Xiang, Qu, Hou and Chen (2011)]. LFM pulse compression signal is utilized worldwide in modern radar system. NLFM signal is a general class of continuous phase coding in which the sweep rate is not restricted to a constant, it is also applied to many kinds of radar systems [Dickey and Holswade (2000)]. In this work, we present a cancelling system for the LFM and NLFM (Taylor window shape [Yichun and Shirui (2005)]) signals. The definition of cancellaty is introduced to measure the effect of active cancellation. Based on the detection probability of radar, we have discussed the scope of the cancellaty.

This paper is organized as follows: in section 2, the approach of LFM and NFLM signals cancelling system is described, and the mathematical formula of cancelling signal is presented. In section 3, we also give the formulas of radar detection probability for moving targets. In section 4, the definition of cancellaty is given, and the effect of amplitude, phased and frequency error on the cancellaty have been investigated. In section 5, the scope of the cancellaty has been studied. In section 6, we provide numerical simulation of the cancelling system. Concluding remarks are given in section 7.

2   LFM and NLFM signal cancelling system

2.1   LFM signal and NLFM signal

An arbitrary FM chirp signal can be expressed as

$$s(t) = a(t)\exp[j\varphi(t)] \tag{1}$$

where $a(t)$ denotes the amplitude modulation function, $\varphi(t)$ denotes the phase modulation function, and the corresponding instantaneous frequency function is

$$f(t) = \frac{1}{2\pi}\frac{d\varphi}{dt} \tag{2}$$

If we suppose the envelope is rectangular, then $a(t) = 1$.

The expression of complex baseband signal of LFM is given by [Wang, Zhao and Wang (2008)]

$$s(t) = \exp(j\pi\mu t^2) \tag{3}$$

where $\mu = B/T$ is called as slope of frequency modulation, B is the bandwidth, T is the pulse duration.

In order to generate the NLFM signal, we should obtain the frequency function $f(t)$ which determines the spectrum shape. In this paper, we consider Taylor window NLFM waveforms as following

$$f(t) = \frac{Bt}{T} - \frac{B}{2} + \sum_{n=1}^{\infty} A(n)B\sin\left(\frac{2\pi nt}{T}\right) \tag{4}$$

where $A(n)$ is the coefficient of the infinite series. In practice, Eq. (4) may be terminated at finite terms. Therefore, the phase function is given by

$$\varphi(t) = \frac{\pi Bt^2}{T} + 2BT\sum_{n=1}^{N} \frac{A(n)}{n}\sin^2\left(\frac{\pi nt}{T}\right) \tag{5}$$

where $N = 10$.

2.2 Model of cancelling signal

The block diagram of the LFM and NLFM signal cancelling system is shown in Figure 1. In Figure 1, $s(t)$ represents the transmitted radar signal, $s_c(t)$ is the cancellation signal, τ_1 is the time delay between the radar signal is received and the cancellation signal is transmitted. $\Delta\tau$ is the jammer processing delay time. On one hand, when the radar signal passes the down conversation, it will be sent to a digital radio frequency memory (DRFM) for storage [Xiang, Qu, Hou and Chen (2011)]. On the other hand, the field programmable gate array (FPGA) chip controls the delay time τ_1 at a particular instant of time t_1, and the received signal is multiplied by the conjugation of its delayed version. Then, multiplying the results to obtain the cancellation signal. Based on the target's RCS, amplitude and phase modulation are made to acquire the signal having the same amplitude and frequency but with the opposite phase [Xiang, Qu, Li and Hou (2013)].
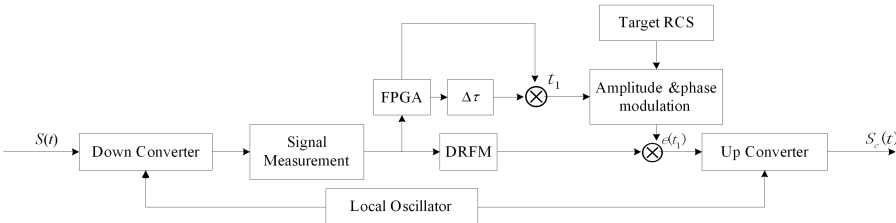

Figure 1: Block diagram of cancellation signal.

The jamming signal $e(t_1)$ is given by

$$e(t_1) = s(t_1) \times s^*(t_1 - \Delta\tau) \cdot a_{RCS} \cdot \exp[j(\phi_{RCS} + \pi)].$$

Let $s(t_1) = s(t - \tau_1)$, the cancellation signal $s_c(t)$ can be given by [Wang, Zhao and Wang (2008)]

$$s_c(t) = s(t - \Delta\tau) \times s(t - \tau_1) \times s^*(t - \tau_1 - \Delta\tau) \times a_{RCS} \times \exp[j(\varphi_{RCS} + \pi)] \qquad (6)$$

where φ_{RCS} and a_{RCS} denote the target's RCS phase and amplitude, respectively. "*" denotes the complex conjugate of the function.

Therefore, substituting Eq. (3) into Eq. (6), we can get the cancellation signal for LFM signal

$$s_c(t) = s(t) a_{RCS} \exp[j(\varphi_{RCS} + \pi)] \exp(-j\pi\mu\tau_1\Delta\tau) \qquad (7)$$

Similarly, substituting Eq. (5) into Eq. (6), we obtain the cancellation signal for Taylor [Xu and Xu (2013)]

$$\begin{aligned} s_c(t) = & s(t) \exp\left(-j\frac{B\pi}{T}\tau_1\Delta\tau\right) \exp\left(-jBT\sum_{n=1}^{N}\frac{A(n)}{n}\cos\left(\frac{n\pi}{T}(\Delta\tau - \tau_1)\right)\right) \times \\ & \exp\left(jBT\sum_{n=1}^{N}\frac{A(n)}{n}\cos\left(\frac{n\pi}{T}(\Delta\tau + \tau_1 - 2T)\right)\right) \times a_{RCS}\exp[j(\varphi_{RCS} + \pi)] \end{aligned}$$

$$(8)$$

3   The detection probability for moving targets using Swerling models

This section discusses the radar detection probability for moving targets using Swerling models. More details can be found in Ref. [Chen, Luo and Chen (2008)].

For Rayleigh probability distribution function of Swerling I and II models

$$f(\sigma) = \frac{1}{\sigma}\exp\left(-\frac{\sigma}{\bar{\sigma}}\right), \quad \sigma \geq 0 \qquad (9)$$

where $\bar{\sigma}$ is the average cross section value. For targets Rayleigh probability distribution function of Swerling III and IV types

$$f(\sigma) = \frac{4\sigma}{\sigma^2}\exp\left(-\frac{2\sigma}{\bar{\sigma}}\right), \quad \sigma \geq 0 \qquad (10)$$

As is known, the radar probability of detection (P_D) is a function of radar the SNR, threshold multiplier and false alarm probability P_{fa}.

Case 1: Detection of Swerling I targets

$$P_{fa} = 1 - \Gamma_1 (V_T, n-1) \tag{11}$$

$$P_D = \begin{cases} \exp[-V_T/(1+SNR)], & n = 1 \\ 1 - \Gamma_1(V_T, n-1) + \left(1 + \frac{1}{n \cdot SNR}\right)^{n-1} \Gamma_1\left(\frac{V_T}{1+\frac{1}{n \cdot SNR}}, n-1\right), & n > 1 \\ \times \exp[-V_T/(1+n \cdot SNR)] \end{cases} \tag{12}$$

where V_T is the threshold voltage when noise alone is present in radar system, n is the number of pulses, $\Gamma_1(x, N) = \int_0^x \frac{\exp(-v)v^{N-1}}{(N-1)!} dv$ is called as incomplete gamma function. For instance, if $P_{fa} = 10^{-6}$, $n = 1, 10, 50, 100$, the relationship between detection probability P_D and SNR is shown in Figure 2.
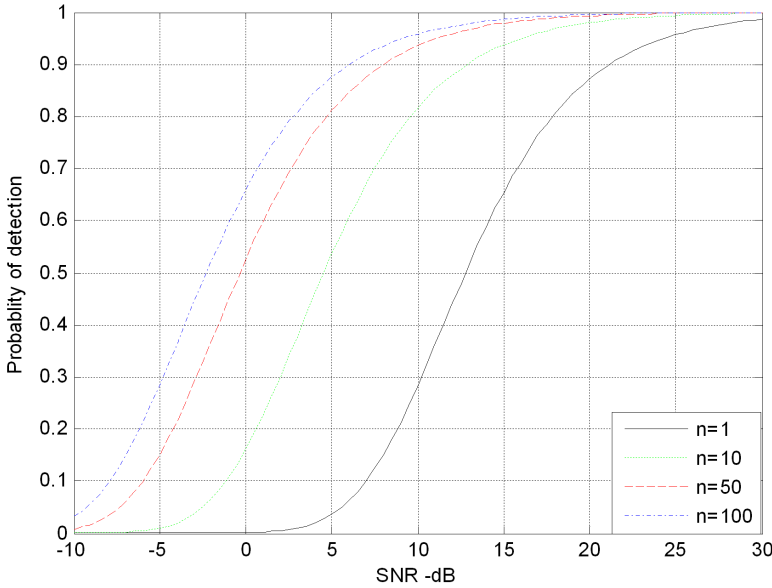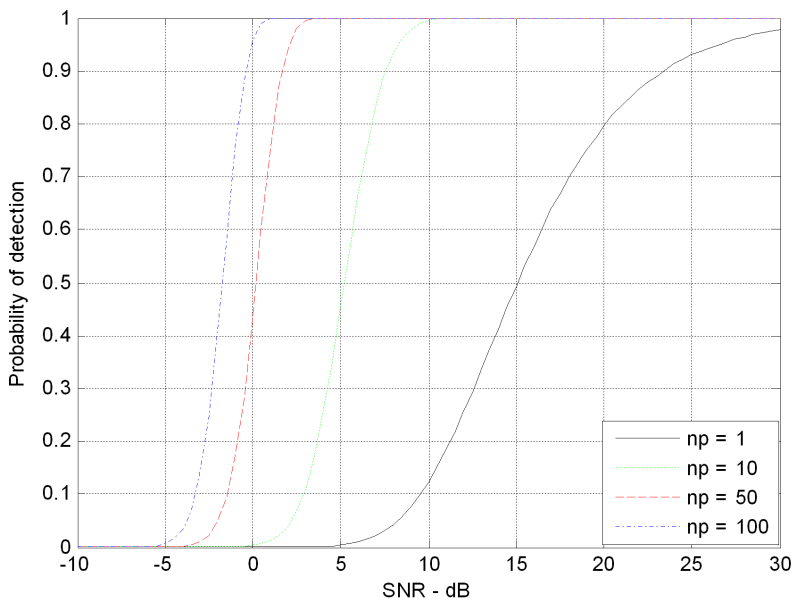

Figure 2: Probability of detection versus SNR for Swerling I type target.

Case 2: Detection of Swerling II targets
When $n \leq 50$, the radar detection probability is

$$P_D = 1 - \Gamma_1\left(\frac{V_T}{1+SNR}, n\right) \tag{13}$$

By using the Gram-Charier series, the radar detection probability can be calculated

as

$$P_D = \frac{erfc(V/\sqrt{2})}{2} - \frac{exp(-V^2/2)}{\sqrt{2}}[c_1(V^2-1)+c_2V(3-V^2)-c_3V(V^4-10V^2+15)]$$

(14)

where the constant c_1, c_2, c_3 are Gram-Charier series coefficients and $V = \frac{V_T - n(1+SNR)}{\varpi}$. The above coefficients and ϖ depend on target fluctuation type. For $n > 50$, the above three coefficients can be obtained as

$$c_1 = -\frac{1}{\sqrt[3]{n}}, \quad c_2 = \frac{1}{4n}, \quad c_3 = \frac{c_1^2}{2}, \quad \varpi = \sqrt{n}(1+SNR).$$

Figure 3 shows the detection probability as a function of SNR for different number of pulses where $P_{fa} = 10^{-10}$ in Swerling model II.

Figure 3: Probability of detection versus SNR for Swerling II type target.

Case 3: Detection of Swerling III targets

The radar detection probability for Swerling III model can be written as

$$P_D = \exp\left(\frac{-V_T}{1+n \cdot SNR/2}\right)\left(1+\frac{2}{n \cdot SNR}\right)^{n-2} \times K_0, \quad n = 1,2$$

(15)

where $K_0 = 1 + \frac{V_T}{1+n\cdot SNR/2} - \frac{2(n-2)}{n\cdot SNR}$. When $n > 2$, we have

$$P_D = \frac{V_T^{n-1}\exp(-V_T)}{(1+n\cdot SNR/2)(n-2)!} + 1 - \Gamma_1(V_T, n-1) + K_0 \times \Gamma_1\left(\frac{V_T}{1+2/n\cdot SNR}, n-1\right)$$
(16)

For instance, if $P_{fa} = 10^{-9}$, $n = 1,\ 10,\ 50,\ 100$, the relationship between detection probability P_D and SNR is shown in Figure 4.
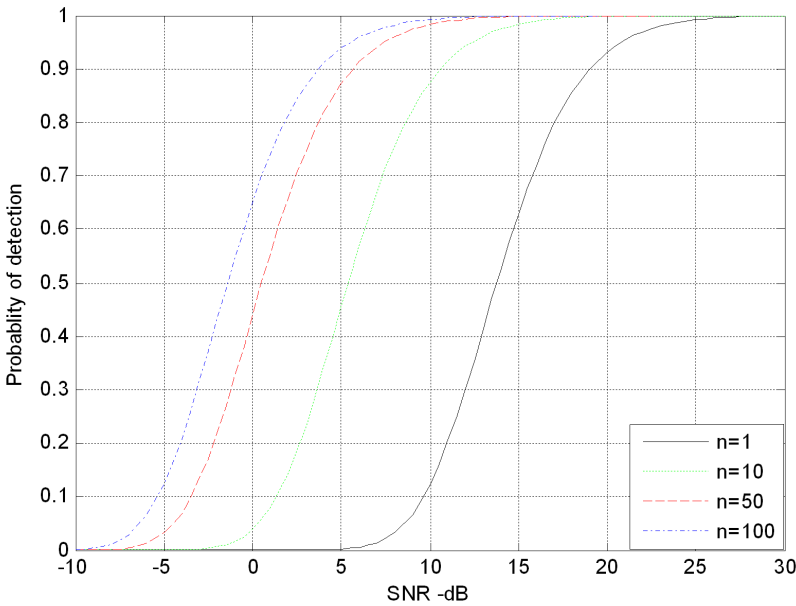

Figure 4: Probability of detection versus SNR for Swerling III type target.

Case 4: Detection of Swerling IV targets

For $n < 50$, the detection probability of Swerling IV target can be expressed as

$$P_D = 1 - \left[\gamma_0 + \left(\frac{SNR}{2}\right)n\gamma_1 + \left(\frac{SNR}{2}\right)^2\frac{n(n-1)}{2!}\gamma_2 + \cdots + \left(\frac{SNR}{2}\right)^2\gamma_n\right]\left(1+\frac{SNR}{2}\right)^{-n}$$
(17)

where $\gamma_i = \Gamma_1\left(\frac{V_T}{1+(SNR)/2}, n+i\right)$.

For $n \geq 50$, the radar detection probability can be computed by using the Gram-Charier series, then we have

$$c_1 = \frac{1}{\sqrt[3]{n}} \frac{2\beta^3 - 1}{(2\beta^2 - 1)^{1.5}}, \quad c_2 = \frac{2\beta^4 - 1}{n(2\beta^2 - 1)^2}, \quad c_3 = \frac{c_1^2}{2},$$

$$\varpi = \sqrt{n(2\beta^2 - 1)}, \quad \beta = 1 + \frac{SNR}{2}.$$

Figure 5 shows the detection probability as a function of SNR for different number of pulses where $P_{fa} = 10^{-9}$ in Swerling model IV.
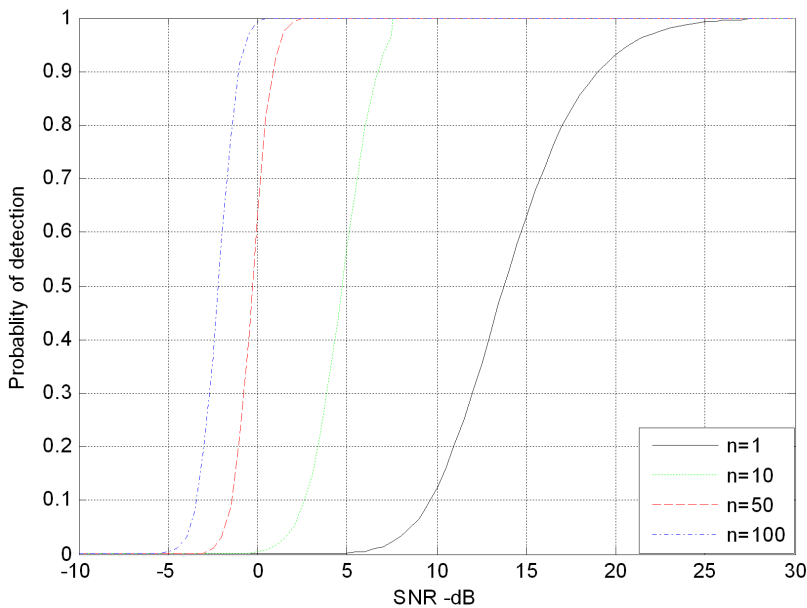

Figure 5: Probability of detection versus SNR for Swerling IV type target.

From the Figure 2-5, we can see clearly that the detection probability becomes large with SNR increasing. With the same value of SNR, the radar detection probability shows more and more large when *n* increases.

4 Concept and analysis of cancellaty

Cancellaty is one of the important parameters which reflect the effect of active cancellation stealth. It is a measurement that shows the cancelled target echo, it also

reflects quantitatively the cancelling function of cancelling echo. The definition is given by

$$S = 20\lg\left(1 + \left|\frac{\Delta e(t)}{s(t)}\right|\right) \tag{18}$$

where $s(t) = Ae^{j\varphi(t)}$, $s_c(t) = A_c e^{j\varphi_c(t)}$, $\Delta e(t) = s(t) - s_c(t) = A_k e^{j\varphi_k(t)}$ is called cancelling echo signal.

According to the properties of complex number, we acquire the expression of amplitude A_k and phase $\varphi_k(t)$ of the cancelling echo signal $\Delta e(t)$.

$$A_k = \sqrt{A^2 - 2AA_c \cos(\varphi(t) - \varphi_c(t)) + A_c^2} \tag{19}$$

$$\tan\varphi_k(t) = \frac{A\sin(\varphi(t)) - A_c \sin(\varphi_c(t))}{A\cos(\varphi(t)) - A_c \cos(\varphi_c(t))} \tag{20}$$

Let $\Delta A = A - A_c$, $\Delta\varphi(t) = \varphi(t) - \varphi_c(t)$, then we have

$$S = 20\lg\left[1 + \sqrt{\left(1 - \frac{\Delta A}{A}\right)^2 - 2\left(1 - \frac{\Delta A}{A}\right)\cos(\Delta\varphi(t)) + 1}\right] \tag{21}$$

In above cancelling system, due to the coherent wave interference principle, the radar echo is completely cancelled out when Eq. (22) are satisfied as follows [Wang, Zhao and Wang (2008)]

$$\begin{cases} \Delta A = 0 \\ \Delta\varphi(t) = 0 \\ \Delta f = 0 \end{cases} \tag{22}$$

where ΔA is the amplitude error, $\Delta\varphi(t)$ is the phase error, and Δf is the frequency error. However, there must be some errors in practical application. When $\Delta\tau$ and τ_1 satisfy some special conditions, the radar echo is cancelled by the interference wave, otherwise the radar echo is strengthened. Next, we will discuss the conditions which satisfy the cancellation. If we consider the frequency error in Eq. (21), Eq. (21) will be transformed as

$$S = 20\lg\left[1 + \sqrt{\left(1 - \frac{\Delta A}{A}\right)^2 - 2\left(1 - \frac{\Delta A}{A}\right)\cos(2\pi\Delta ft + \Delta\varphi) + 1}\right] \tag{23}$$

If we take $\Delta A = 0$, $\Delta\varphi = 0$, then the cancellaty versus Δf becomes

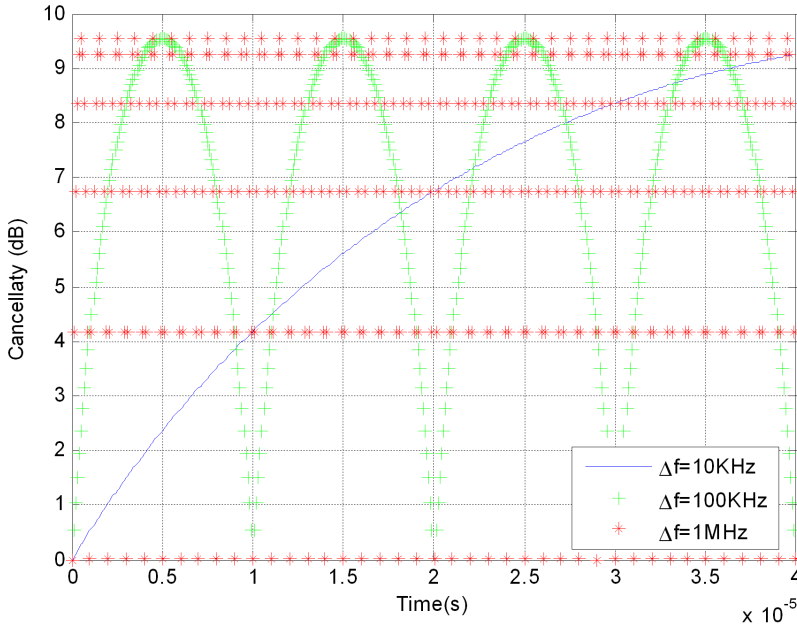$$S_{\Delta f} = 20\lg\left[1 + 2\left|\sin(\pi\Delta ft)\right|\right] \tag{24}$$

Figure 6: Cancellaty versus frequency error.

Figure 6 shows how the cancellaty vary with frequency error. From the Figure 6, we find that the cancellaty shows periodic change. The bigger the frequency error is, the shorter the periodic.

Similarly, if $\Delta f = 0$, $\Delta \varphi = 0$, then the cancellaty versus ΔA can be written as

$$S_{\Delta A/A} = 20 \lg \left[1 + \left| \frac{\Delta A}{A} \right| \right] \tag{25}$$

Figure 7 shows how the cancellaty vary with amplitude error. Likewise, if $\Delta f = 0$, $\Delta A = 0$, then the cancellaty versus $\Delta \varphi$ can be expressed as

$$S_{\Delta \varphi} = 20 \lg \left[1 + 2 \left| \sin \left(\frac{\Delta \varphi}{2} \right) \right| \right] \tag{26}$$

Figure 8 shows how the cancellaty vary with phase error. Let $a_{RCS} = 1$ and $\phi_{RCS} = 0$ as the simplified form, then we can also derived the relationship between $\Delta \varphi$ and τ_1, $\Delta \tau$ from Eq.(7) and Eq.(8), the corresponding expressions are given by
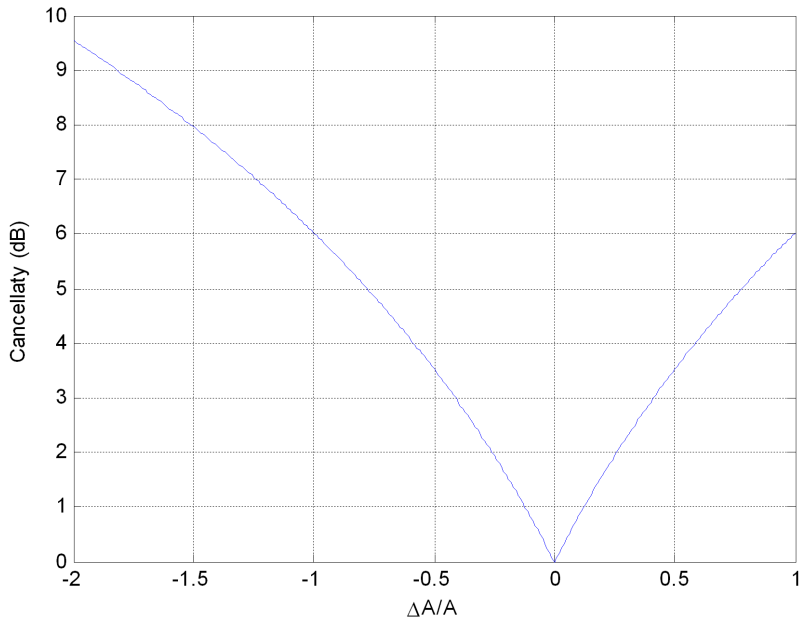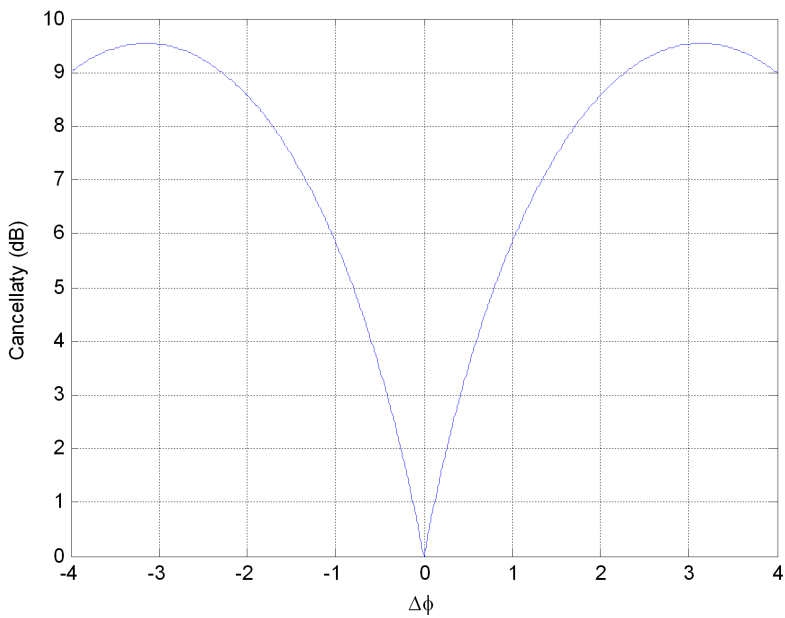
Figure 7: Cancellaty versus amplitude error.

Figure 8: Cancellaty versus phase error.

(I) Linear frequency modulated (LFM)

$$\Delta\varphi = \pi\mu\tau_1\Delta\tau + \pi \tag{27}$$

(II) Nonlinear frequency modulated (NLFM) for Taylor window shape

$$\Delta\varphi = \frac{B\pi}{T}\tau_1\Delta\tau + BT\sum_{n=1}^{N}\frac{A(n)}{n}\cos\left(\frac{n\pi}{T}(\Delta\tau - \tau_1)\right)$$
$$- BT\sum_{n=1}^{N}\frac{A(n)}{n}\cos\left(\frac{n\pi}{T}(\Delta\tau + \tau_1 - 2T)\right) + \pi \tag{28}$$

From Figure 6-8, we see clearly that the cancellaty is changing with different values of $\Delta A/A$, $\Delta\varphi$ and Δf. The cancellaty $S = 0$ if and only if $\Delta A = 0$, $\Delta\varphi = 0$ and $\Delta f = 0$. However, in practical, ΔA, $\Delta\varphi$ and Δf are not equal to zero, we are unable to determine the extent of the cancellation by taking a closer Figure 6-8. In other words, from the Figure 6-8, we don't know when the cancelling wave cancels the radar echo, and when it strengthens the radar echo. Consequently, we should give a scope of cancellaty to illustrate when the radar echo is completely cancelled out, when the radar echo is mostly cancelled out, and when it is strengthened. Next, we will apply the detection probability of radar in Section 3 to solve these problems.

5 The discussion about the scope of cancellaty using detection probability of radar

According to the definition of SNR, we can approximately obtain the improved SNR of the radar echo after adopting the cancelling system, it may be written as

$$SNR_L = (10^{S/20} - 1)^2 \cdot SNR \tag{29}$$

Substituting Eq. (29) into Eq. (12)~Eq. (17), we get the cancelled detection probability of radar versus S, which are shown in Figure 9-12, In Figure 9-12, we take $SNR = 30$.

From Figure 9-12, we see that the detection probability of radar vary with different S. Based on the detection probability of radar, we can derive the scope of cancellaty S.

In addition, when $SNR = 30$, from Figure 2-5 we can obtain the detection probability of radar which are expressed in Table 1. After applying the active cancellation technique, the detection probability of radar will decrease. Then we will discuss the extent of cancellation by using the detection probability of radar, and derive correspondingly the scope of cancellaty.

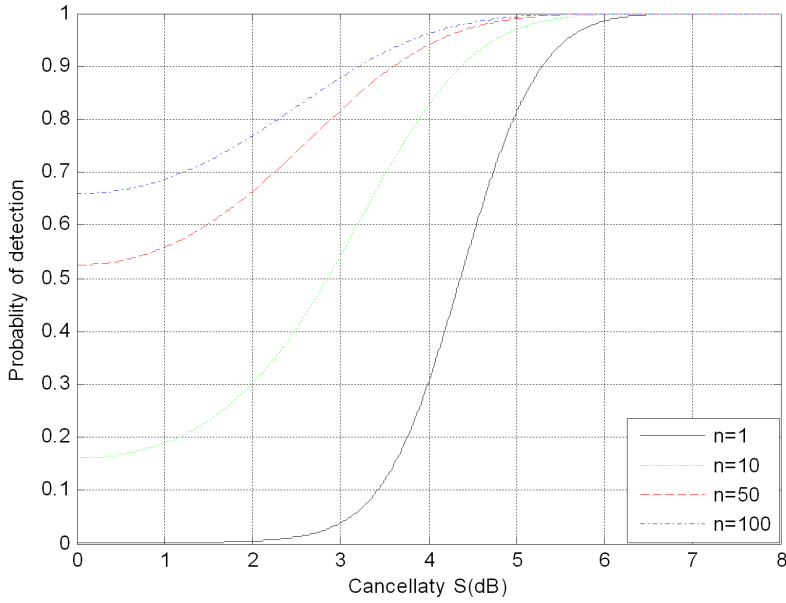**Case 1:** The radar echo is partly cancelled out.

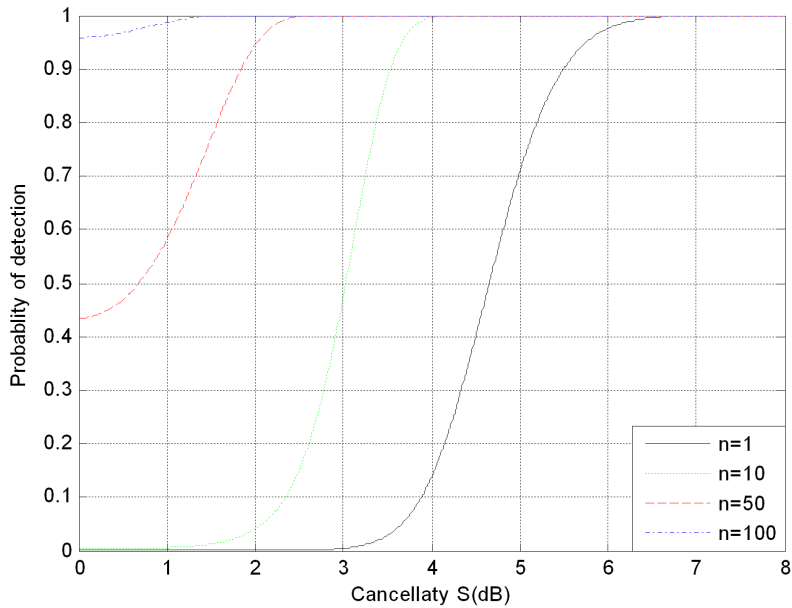Figure 9: Probability of detection versus cancellaty for Swerling I type target.

Figure 10: Probability of detection versus cancellaty for Swerling II type target.
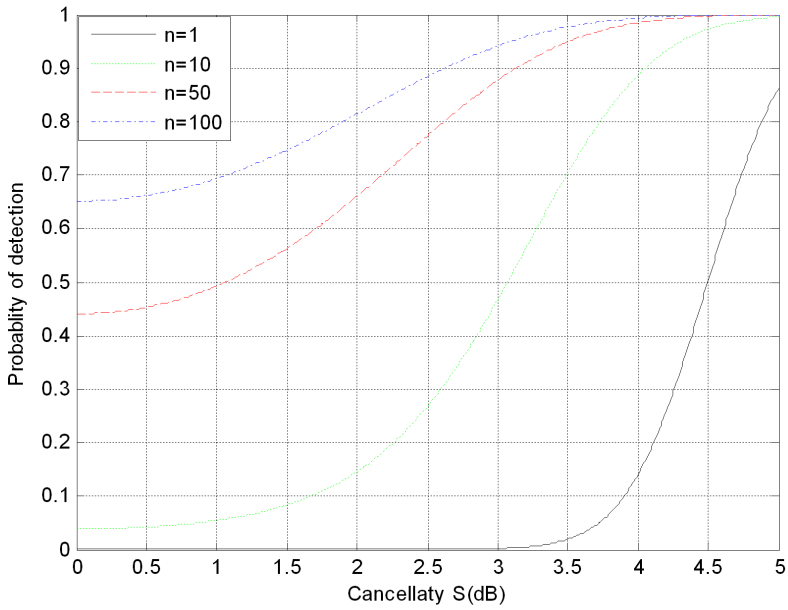
Figure 11: Probability of detection versus cancellaty for Swerling III type target.
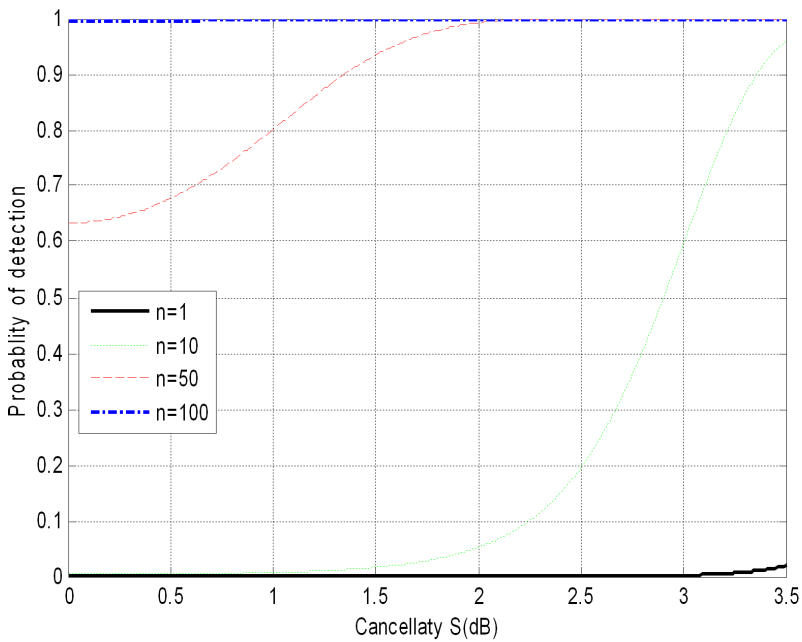

Figure 12: Probability of detection versus cancellaty for Swerling IV type target.

Table 1: Detection probability of radar versus n for different Swerling type targets.

Model	$n = 1$	$n = 10$	$n = 50$	$n = 100$
Swerling I	98.63%	99.79%	99.93%	99.96%
Swerling II	97.73%	100%	100%	100%
Swerling III	99.91%	99.99%	100%	100%
Swerling IV	99.91%	100%	100%	100%

Table 2: The scope of cancellaty for partial cancellation.

| Model	$n = 1$	$n = 10$	$n = 50$	$n = 100$
Swerling I	[0, 6.03]	[0, 6.03]	[0, 6.03]	[0, 6.05]
Swerling II	[0, 6.03]	[0, 5.63]	[0, 3.74]	[0, 4.05]
Swerling III	[0, 6.03]	[0, 5.74]	[0, 5.43]	[0, 5.13]
Swerling IV	[0, 6.03]	[0, 3.55]	[0, 3.13]	[0, 2.51]

When the detection probability of radar falls below the value of Table 1, we may consider the radar echo is cancelled out. At this moment, we can obtain correspondingly the scope of cancellaty which are shown in Table 2.

**Case 2:** The radar echo is completely cancelled out.

According to the above discussion in Section 4, the radar echo is completely cancelled out when the cancellaty $S = 0$. However, in actual radar countermeasure, it is usually difficult to detect target when the detection probability of radar falls below 50%, and therefore there is no need to cancel the echo signal completely. We may consider the echo is completely cancelled out when the corresponding detection probability of radar falls below 50%. At this time, we can get the scope of cancellaty which are shown in Table 3.

Table 3: The scope of cancellaty for complete cancellation.

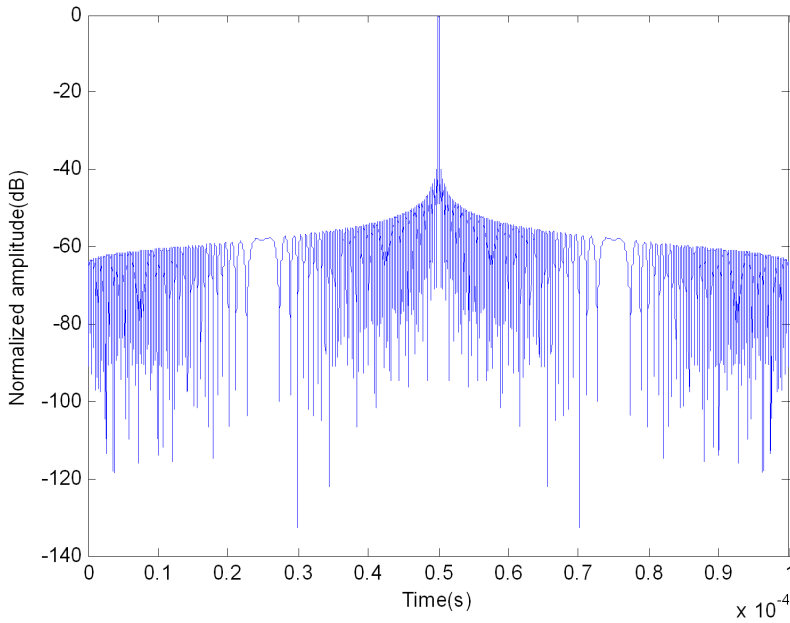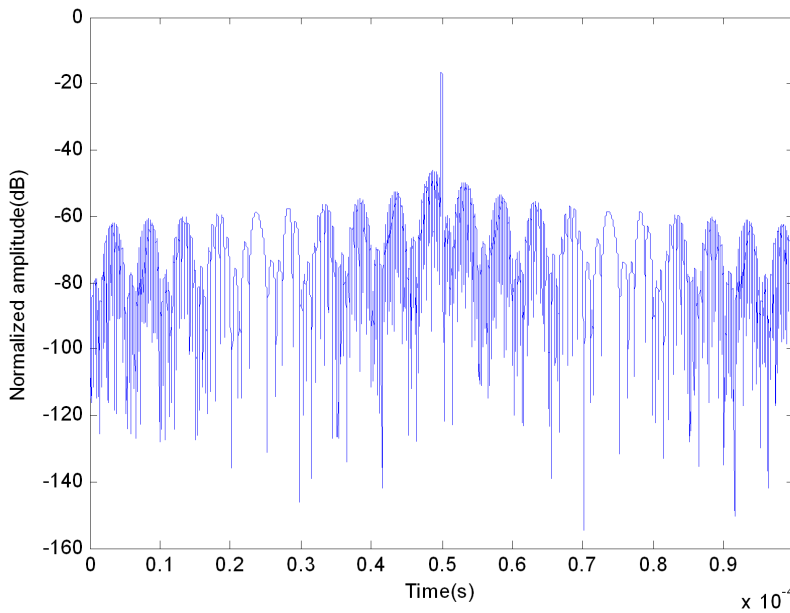| Model	$n = 1$	$n = 10$	$n = 50$	$n = 100$
Swerling I	[0, 4.37]	[0, 2.86]	–	–
Swerling II	[0, 4.66]	[0, 3.03]	[0, 0.69]	–
Swerling III	[0, 4.50]	[0, 3.07]	[0, 1.07]	–
Swerling IV	[0, 4.50]	[0, 2.91]	–	–
"–" denotes nothingness.				
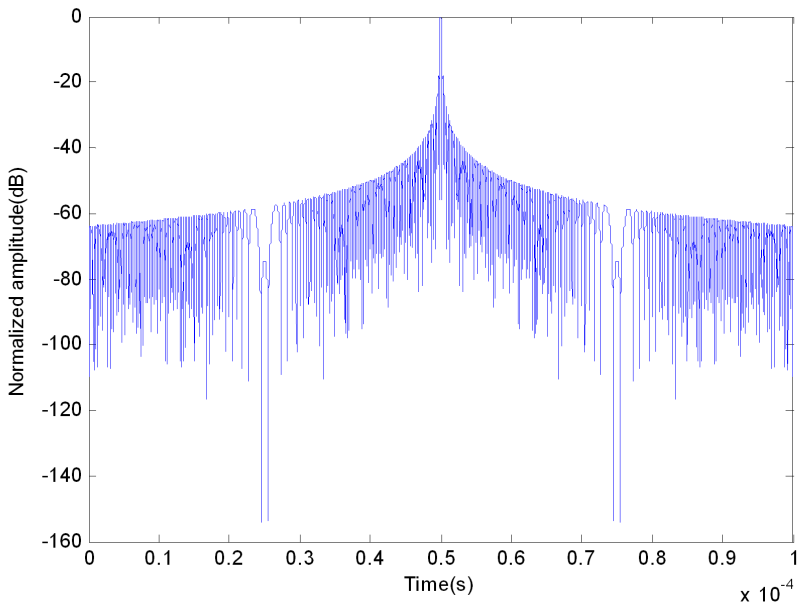
(a)
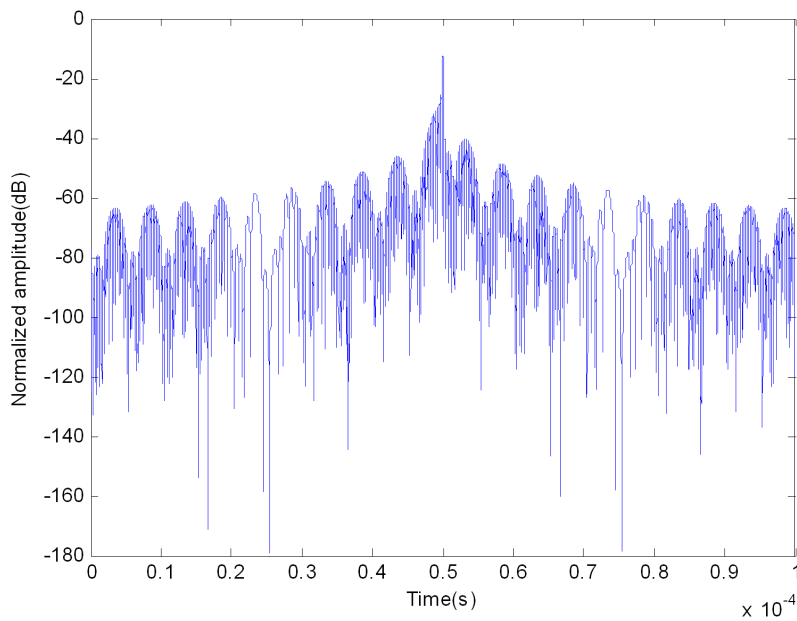
(b)

Figure 13: (a) Before cancelling echo signal for LFM; (b) After cancelling echo signal.

(a)

(b)

Figure 14: (a) Before cancelling echo signal for Taylor window shape NFLM; (b) After cancelling echo signal for Taylor window shape NFLM.

From Table 2 and Table 3, we conclude that the scope of cancellaty becomes smaller and smaller with n increasing.

Case 3: The radar echo is strengthened.

When the detection probability of radar exceeds the value of Table 1, the cancelling system will strengthen the radar echo. We must try to avoid this kind of circumstance happening.

6   Simulation of the cancelling system

In this section, simulation experiments are carried out to illustrate the effect of active cancellation stealth for LFM and NFLM signal. The parameters are set as follows: impulse width for LFM and NLFM signals is $50\mu s$, bandwidth is 10MHz, the ratio interference to echo amplitude (amplitude error) is 0.4, frequency error is 1KHz, delay time is $2\mu s$. The simulation results are shown in Figure 13 and Figure 14.

The simulation results show that using the above cancelling system can reduce the echo gain. Under error conditions, the system still has a very high cancellation effect. From the Figure 13(b), the signal amplitude is decreased about 15dB. From the Figure 14(b), the signal amplitude is also decreased about 18dB.

7   Conclusion

The radar detection probability is controlled effectively and efficiently through interaction between the cancellation signal and echo signal. The definition of cancellaty is proposed to illustrate the effectiveness of the cancelling system. Using the radar detection probability and cancellaty, the extent of active cancellation can be classified as partial cancellation, complete cancellation and strengthening echo. The simulation results also indicate that the echo gain can be reduced by using the cancelling system. Even though there exists some errors, the system still has very high interference effect.

References

Cecchi, S.; Romoli, L.; Peretti, P.; Piazza, F. (2012): Low-complexity implementation of a real-time decorrelation algorithm for stereophonic acoustic echo cancellation. *Signal Processing*, vol. 92, pp. 2668-2675.

Chen, Z. J.; Luo, Q.; Chen, Q. (2008): *Radar Systems Analysis and Design Using MATLAB Second Edition*, Publishing House of Electronics Industry, Beijing.

Dickey, F. M.; Holswade, C. S. (2000): *Laser Beam Shaping Theory and Techniques*, Marcel Dekker Inc., New York.

Guo, X.; Sun, H. B.; Yeo, T. S. (2008): Interference cancellation for high frequency surface wave radar. *IEEE Transactions on Geosciences and Remoter Sensing*, vol. 46, no. 7, pp.1879- 1892.

lizuka, K.; Freundorfer, A. P.; Iwasaki, T. (1989): A method of surface clutter cancellation for an under- ground CW radar. *IEEE Transactions on Electromagnetic Compatibility*, vol. 31, no. 3, pp. 330-332.

Jenn, D. C. (2005): *Radar and Laser Cross Section Engineering*. American Institute of Aeronautics and Astronautics Inc.

Kay, S.; Boudreaux-Bartels G. (1985): On the optimality of the Winger distribution for detection. IEEE Acoustics. *Speech, and Signal Processing* , pp. 1017-1020.

Lynch, D. (2004): *Introduction to RF stealth*. Raleigh: SciTech Publishing.

Mauro, A. A.; Rafael, J. P.; Mirabel, C. R. (2007): Simulations of the radar cross section of a stealth aircraft. *IEEE International Microwave and Optoelectronics Conference*, Brazil.

Paleologu, C.; Benesty, J.; et.al. (2014): Widely linear general Kalman filter for stereophonic acoustic echo cancellation. *Signal Processing*, vol.94, pp. 570-575.

Qu, C. W.; Xiang, Y. C. (2010): Active Cancellation Stealth Analysis Based on RCS Characteristic of Target. *Radar Science and Technology*, vol. 8, no. 2, pp. 109-112.

Qu, C. W.; Xiang, Y. C.; Hou, H. P.; Zhou, W. J. (2011): Cancellation Interference Analysis of Coherent Radar Based on Phase Modulation. *Journal of University of Electronic Science and Technology of China*, vol. 40, no. 6, pp. 829-834.

Root, B. (1998): HF radar ship detection through clutter cancellation. *IEEE National Radar Conference*, Dallas, pp. 281-286.

Stanciu, C.; Benesty, J. et.al. (2013): A widely linear model for stereophonic acoustic echo cancellation. *Signal Processing*, vol. 93, pp. 511-516.

Wang, Y. J.; Zhao, G. Q.; Wang, H. W. (2008): Echo cancelling algorithm for the LFM radar. *Journal of Xidian University*, vol. 35, no. 6, pp. 1031-1035.

Xiang, Y. C.; Qu, C. W.; Li, B. R.; Hou, H. P. (2013): Simulation Research on Cancellation Stealth of Warship Based on Its Radar Scattering Properties. *Journal of System Simulation*, vol.25, no.1, pp.104-110.

Xiang, Y. C.; Qu, C. W.; Ping, D. F.; Zhao, W. Q. (2010): Research on Active Cancellation Stealth of Warship. *Ship Electronic Engineering*, vol. 30, no. 2, pp. 103-106.

Xiang, Y. C.; Qu, C. W.; Hou, H. P.; Chen, Y. K. (2011): Analysis of LFMICW Cancellation Based on Group Delay and Ambiguity Function. *Journal of CAEIT*, vol. 6, no. 2, pp. 175-180.

Xu, S.; Xu, Y. M. (2013): Scheme for nonlinear frequency modulation signal cancelling system. *Optik*, vol. 124, no. 21, pp. 4896-4900.

Yichun, P.; Shirui, P.; et.al. (2005): Optimization design of NLFM signal and its pulse compression simulation. *IEEE Int. Conf. Radar, Arlington*, pp. 383-386.